PROCEEDINGS, Twenty-First Workshop on Geothermal Reservoir Engineering
Stanford University, Stanford, California, January 22-24, 1996
SGP-TR-151

# NUMERICAL SIMULATION OF ELECTROKINETIC POTENTIALS ASSOCIATED WITH SUBSURFACE FLUID FLOW

**Tsuneo Ishido[+] and John W. Pritchett[++]**

**[+] Geological Survey of Japan, 1-1-3 Higashi, Tsukuba, 305 Japan**

**[++]S-Cubed, La Jolla, California**

## ABSTRACT

A postprocessor has been developed to calculate space/time distributions of electrokinetic potentials resulting from histories of underground conditions (pressure, temperature, flowrate, etc.) computed by multi-phase multi-component unsteady multidimensional geothermal reservoir simulations. Electrokinetic coupling coefficients are computed by the postprocessor using formulations based on experimental work reported by Ishido and Mizutani (1981). The purpose of the present study is to examine whether or not self-potential anomalies actually observed in real geothermal fields are consistent with quantitative mathematical reservoir models constructed using conventional reservoir engineering data. The most practical application of the postprocessor appears to be modeling self-potential changes induced by field-wide geothermal fluid production. Repeat self-potential surveying appears to be promising as a geophysical monitoring technique to provide constraints on mathematical reservoir models, in a similar fashion to the use of repeat microgravity surveys.

## INTRODUCTION

A self-potential (SP) survey is conducted by mapping the natural time-invariant electric field at the earth's surface. In recent years, the SP method has attracted increasing interest in geothermal prospecting and engineering geophysics. Among the various mechanisms which can cause SP, the most important appear to be electrokinetic (streaming) potentials arising from underground fluid flow (e.g., Ogilvy et al., 1969; Zohdy et al., 1973; Combs and Wilt, 1976; Zablocki, 1976; Anderson and Johnson, 1976; Mizutani et al., 1976; Corwin and Hoover, 1979; Ishido, 1989; Ishido et al., 1987; 1990).

In general, electrokinetic effects have been described on the basis of irreversible thermodynamics (de Groot and Mazur 1962). There are, however, several difficulties involved in quantitative interpretation of electrokinetic effects in the earth. First, in-situ values of the cross-coupling coefficients (zeta potential and/or streaming potential coefficient) are hard to estimate. This difficulty has been partially alleviated by experimental studies of the zeta potential and streaming potential coefficient for crustal rock-water systems (Ishido and Mizutani, 1981; Ishido et al., 1983; Morgan et al., 1989).

Quantitative SP interpretation is difficult because of the complicated character of SP generation by subsurface electrokinetic sources. Theoretical studies by Nourbehecht (1963), Fitterman (1978), Ishido (1981; 1989), and Sill (1983) have helped to explain these processes. Numerical modeling of SP has also been undertaken recently, following Sill's approach (Yasukawa et al., 1993; Wurmstich and Morgan, 1994).

In this paper, we describe a newly developed postprocessor which calculates electrokinetic potentials based upon multidimensional unsteady computed histories of underground conditions computed by the "STAR" general-purpose geothermal reservoir simulator (Pritchett, 1989; see also Pritchett, 1995). The results of numerical modeling of natural SP anomalies in geothermal fields and production-induced SP changes are also presented.

## ELECTROKINETIC MECHANISMS OF SELF-POTENTIAL GENERATION

The flow of a fluid through a porous medium may generate an electrical potential gradient (called the electrokinetic or streaming potential) along the flow

path by the interaction of the moving pore fluid with the electrical double layer at the pore surface. This process is known as electrokinetic coupling. The general relations between the electric current density **I** and fluid volume flux **J** (on the one hand), and the electric potential gradient $\nabla\phi$ and pore pressure gradient $\nabla\xi$ forces (on the other) are

$$\mathbf{I} = - Lee\nabla\phi - Lev\nabla\xi \; ; \qquad (1)$$

$$\mathbf{J} = - Lve\nabla\phi - Lvv\nabla\xi \; ; \qquad (2)$$

where the Lab are phenomenological coefficients. The first term on the right-hand side in Eq. 1 represents Ohm's law and the second term in Eq. 2 represents Darcy's law. The cross-coupling terms (with the Lev and Lve coefficients) represent the electrokinetic effect; Lev = Lve according to Onsagar's reciprocal relations.

Eq. 1 describes the total current density, composed of a drag (convection) current density **Idrag** caused by charges moved by fluid flow, and a conduction current density **Icond** caused by electric conduction; hence,

$$\mathbf{I} = \mathbf{Icond} + \mathbf{Idrag} \qquad (3)$$

where

$$\mathbf{Icond} = -Lee\,\nabla\phi$$

$$\mathbf{Idrag} = -Lev\,\nabla\xi$$

In the absence of external current sources, $\nabla \mathbf{I} = 0$, so from Eq. 3:

$$\nabla\,\mathbf{Icond} = -\nabla\,\mathbf{Idrag} \qquad (4)$$

Eq. 4 represents sources of conduction current which are required for the appearance of electric potential at the surface.

The cross-coupling term of Eq. 2 is negligible; the maximum value of the induced electric potential (streaming potential) is given as $\nabla\phi = - Lev/Lee\,\nabla\xi$ from Eq. 1 assuming $\mathbf{I} = 0$. Substituting this value into Eq. 2 yields:

$$\mathbf{J} = - Lvv\,(1 - Lev^2/Lee\,Lvv)\nabla\xi \; ,$$

where the quantity $Lev^2/Lee\,Lvv$ is $O(10^{-5})$ for typical geologic situations and may be safely neglected. Thus, Darcy's law alone may be used to model the hydraulic problem; it is not necessary to solve Eqs. 1 and 2 simultaneously. A "postprocessor" may then be used to calculate the drag current (**Idrag**) from the results of an unsteady thermohydraulic reservoir simulation.

## EKP-POSTPROCESSOR

Our postprocessor simulates electric potentials caused by subsurface fluid flow by a two-step process. First, it calculates the distribution of Idrag (and $\nabla$ Idrag ) and Lee from the reservoir-simulation results using the same spatial grid used for the reservoir simulation calculation (called the RSV-grid hereafter). This process is explained in detail below. Next, the postprocessor calculates the electric potential ($\phi$) distribution by solving Eq. 4 within a finite-difference grid which is usually much greater in spatial extent than the RSV-grid (hereafter called the SP-grid). The relationship between the RSV- and SP- grids is depicted in Fig. 1.

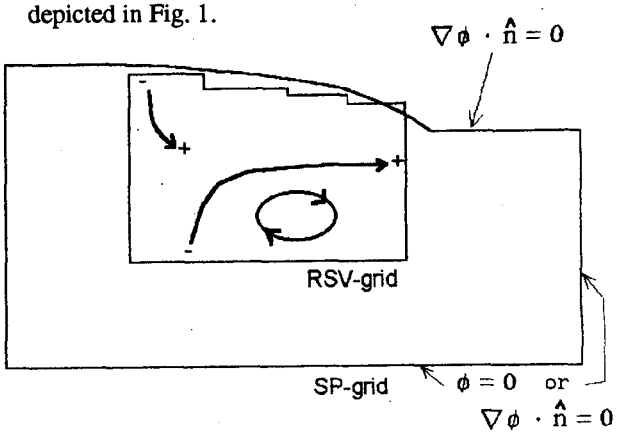


Fig. 1 Relationship between RSV- and SP- grids.

Within that portion of the SP-grid overlapped by the RSV-grid, the distribution of electrical conductivity is obtained directly from RSV-grid values (see above). Elsewhere within the SP-grid, the electrical conductivity distribution is user-specified and time-invariant. Ordinarily, boundary conditions on the potential are: zero normal gradient on the ground surface (upper surface) and zero potential along the bottom and vertical sides of the SP-grid. It is also possible to prescribe zero normal gradient on all exterior surfaces of the SP-grid. Eq. 4 is solved numerically using a Gauss-Seidel iteration procedure which incorporates intermittant automatic optimization of the overrelaxation factor.

The drag current density within the RSV-grid is given by:

$$\mathbf{Idrag} = - Lev\; M_L v_L / kR_L \qquad (5)$$

where $M_L$ , $v_L$ and $R_L$ are the mass flux density, kinematic viscosity and relative permeability of liquid

phase, respectively, and k is the absolute permeability (which is the local instantaneous value used in the reservoir simulator, subject to the constraint that k must exceed a user-supplied kmin value which may be a function of position).

The coupling coefficient is computed based upon the capillary model described by Ishido and Mizutani (1981),

$$Lev = -\eta t^{-2} G Rev \epsilon \zeta / \mu_L \qquad (6)$$

where $\eta$ and t are the porosity and tortuosity of the porous medium; $\epsilon$ and $\mu_L$ are the dielectric permittivity and dynamic viscosity of the liquid phase; and $\zeta$ is the zeta potential, the potential across the electrical double layer. If $\zeta$ is negative (positive), positive (negative) charge is carried by the fluid flow **J**. The G and Rev factors are newly introduced: G ($\leq$ 1) is a correction factor in cases of very small hydraulic radius (comparable to the thickness of the electrical double layer) and Rev ($\leq$ 1) is a user-specified function of the liquid-phase saturation.

The zeta-potential in Eq. 6 is a function of temperature, pH and the concentration of 1:1 and 2:2 valent electrolyte in the solution, and is given by Eqs. 18, 20 and 21 of Ishido and Mizutani's paper (1981) assuming the following empirical relation for the distance (Xs) between the solid surface and the slipping plane in the electrical double layer,

$$Xs \text{ (meters)} = 3.4\times10^{-6} \ \mu_L \text{ (pascal-seconds)}$$

In the present version of the postprocessor, pH ($\Delta$ pH) must be supplied by the user as a function of position. The effects of $Al^{+++}$ ion on $\zeta$ can also be taken into account. The dielectric permittivity $\epsilon$ is given as a function of temperature and pressure (and, if desired, the concentration of dissolved species; see e.g., Olhoeft, 1981).

The electrical conductivity of the bulk fluid/rock composite (Lee) is calculated from the porosity and the conductivity of the rock matrix ($\sigma_R$) and the pore fluid ($\sigma_F$). Several types of "mixing law" are available in the postprocessor, such as Archie's law and the capillary model. The pore fluid conductivity is also calculated as the effective composite conductivity of liquid, vapor and solid salt phases in the pores using one of several user-selected mixing laws. The liquid-phase conductivity is a function of temperature, pressure, and the concentrations of NaCl, KCl and $CaCl_2$ based on the formulation given in Olhoeft (1981) (the coefficients of the formulation were corrected using the original data of Quist and Marshall, 1968).

## ILLUSTRATIVE CASE 1: SINGLE-PHASE GEOTHERMAL RESERVOIR

We will describe two illustrative computations using the computational/graphical EKP postprocessor. The first is a simple model which simulates natural hydrothermal convection and production/reinjection effects. The second (described in the next section) is based on a three-dimensional thermohydraulic model originally developed to represent the natural-state of the Sumikawa geothermal reservoir (Pritchett et al., 1991).

A two-dimensional computational grid was used in the first model; it consists of 20 grid blocks in the horizontal direction and 10 grid blocks in the vertical direction (each block is 200 m x 200 m in size). All exterior boundaries except the top surface are closed; pressure and temperature are maintained at 1 bar and 20 °C respectively along the top boundary. Any "fresh water" which flows downward into the grid through the top surface contains a dilute tracer to permit its identification.

A source of high-temperature "magmatic water" (similarly tagged with a dilute tracer) was imposed at the center of the grid bottom; the evolution of the hydrothermal convection system was then simulated using the STAR simulator. The system reached steady state after about $10^4$ years; in Fig. 2, the distributions of temperature, fluid mass flux and mass fraction of "magmatic dilute tracer" are shown for $10^5$ years.

For the self-potential calculations, the magmatic fluid is assumed to contain NaCl and $Al^{+++}$; the concentrations are proportional to the mass fraction of magmatic dilute tracer, and NaCl and $Al^{+++}$ are 0.17 mol/l and $1.2\times10^{-5}$ mol/l respectively in the pure upflowing magmatic fluid entering from below. The fresh water is assumed to contain only dilute NaCl ($1.7\times10^{-3}$ mol/l). The postprocessor calculates Lee, Lev and $\nabla$ Idrag from these distributions of composition and other results from the STAR simulation (such as temperature, pressure and fluid mass flux) within the RSV-grid. Then the distribution of electric potential is calculated within the SP-grid; the results are shown in Fig.3.

A positive self-potential anomaly is present above the upflow region. This is brought about by positive sources of conduction current; $\nabla$Icond (=-$\nabla$ Idrag) has maxima at 300 m depth in the central upflow region. The $\zeta$-potential changes from about -50 mV (at 2 km depth) to near 0 mV (in the uppermost block) with decreasing temperature in the upflow region. This is

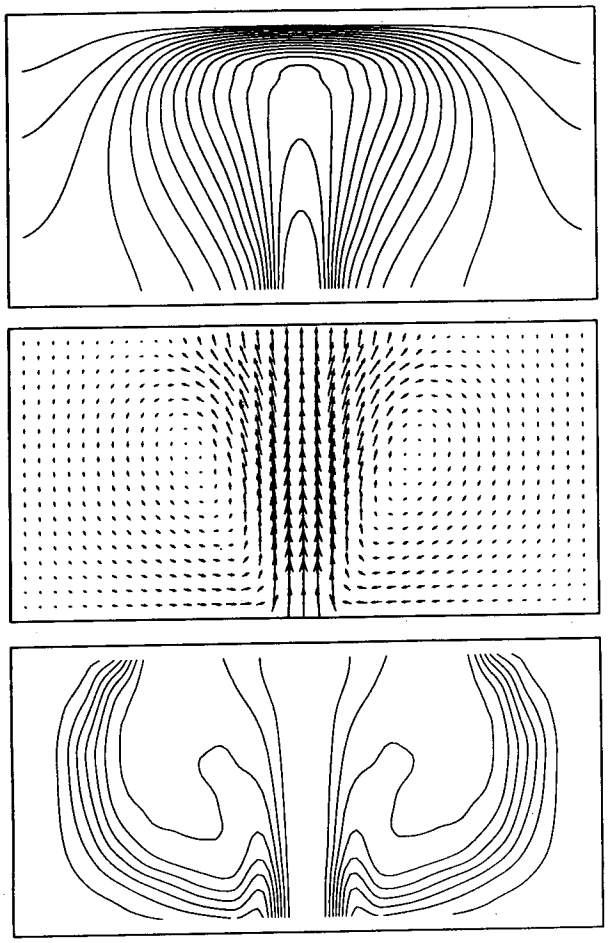

Fig. 2. Natural-state distributions of temperature (contour interval is 10 °C), fluid mass flux and mass fraction of "magmatic dilute tracer" (contour interval is 10 %) are shown in top, middle and bottom diagrams respectively.

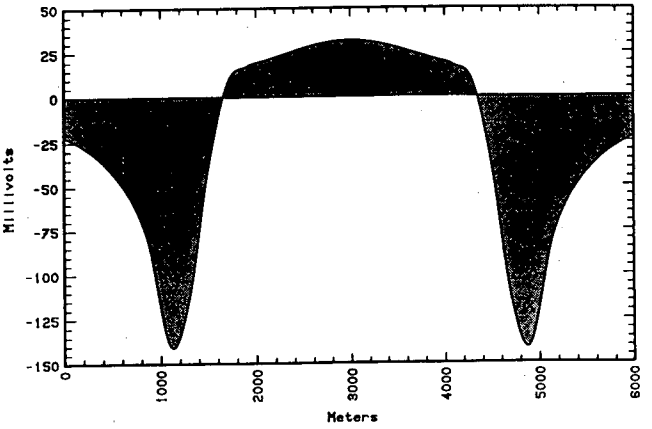


Fig. 3. Calculated self-potential distribution for the natural state (Fig. 2).

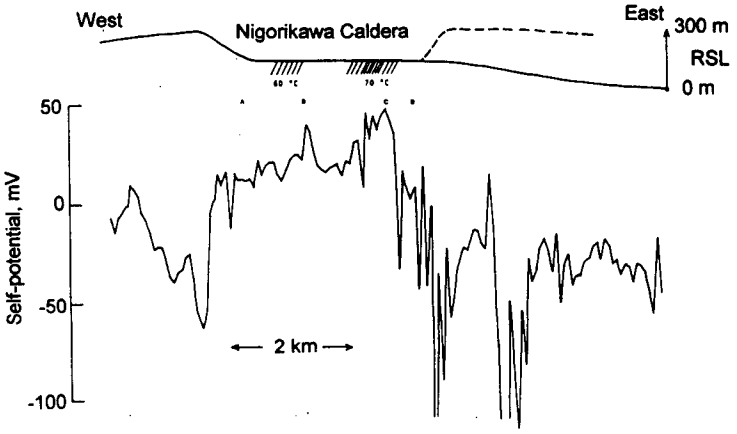


Fig. 4. Topographic section and self-potential profile across the Nigorikawa caldera in 1978 (after Ishido, 1981).

the main cause of positive-charge accumulation along the upflow path.

Large negative anomalies appear in the region where meteoric water flows downward. The descending meteoric water removes positive charge from the neighborhood of the ground surface and thus produces a conduction current sink. The peripheral negative anomalies are larger in magnitude than the central positive anomaly due to relatively low electrical conductivity (about 0.01 S/m in the down-flow region compared to 1 S/m in the upflow region).

A representative flow rate (Darcy velocity) is $10^{-8}$ m/s in the present case. If the flow rate is increased by prescribing a hotter "magmatic" fluid source, the magnitudes of both the positive and negative anomalies will increase. The results of the present calculation confirm the "semi-quantitative" prediction by Ishido (1981; see also Ishido et al., 1987). Fig. 4 shows the measured self-potential profile across the Nigorikawa caldera (Ishido, 1981), an active geothermal field located in Hokkaido, Japan. SP is high inside the caldera (where the upflows take place which charge the field), but the surrounding area is characterized by negative SP anomalies. These features are well reproduced in the present simple model (Fig. 3).

In the Nigorikawa caldera, the Mori geothermal power plant was built in 1982 and has been in continuous operation since. Comparing the results of SP surveys in 1978, 1981 and 1984, Ishido et al. (1987) found a production-induced SP change. The most obvious change took place in the eastern part of the caldera; a decrease in SP of about 40 mV was observed along the eastern caldera rim.

We also calculated the SP distribution assuming production and reinjection in the present model. Although the flow pattern is dominated by production-induced flow, the SP distribution pattern

under exploitation is very similar to the natural-state (compare Fig. 5 to Fig. 3). The only substantial change occurs in the (negative potential) peripheral downflow ranges, where the magnitude of the anomalies increases from -150 mV in the natural state to -250 mV under production conditions. (This mechanism can be interpreted based upon the total potential approach presented by Nourbehecht, 1963; see also Fitterman, 1978) These trends are consistent with field observations of SP changes at Mori.

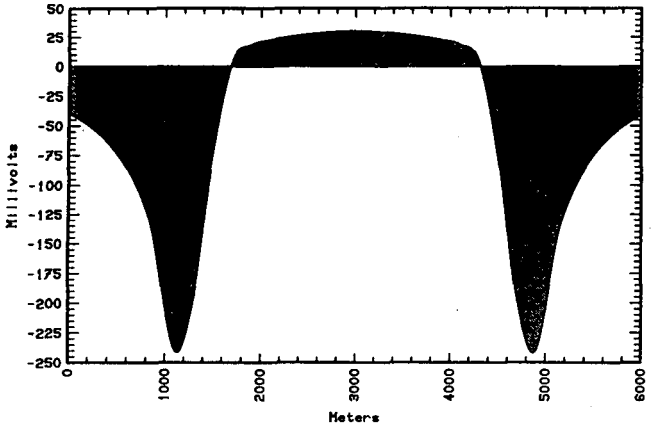


Fig. 5. Calculated self-potential distribution assuming production and reinjection in the model shown in Fig. 2. The result after 5 years of operation is shown.

## ILLUSTRATIVE CASE 2: THE SUMIKAWA GEOTHERMAL FIELD

We next applied the EKP postprocessor to a detailed 3-dimensional model of the Sumikawa field (Pritchett et al., 1991); the SP distribution was calculated both for the "natural-state" (Fig. 6(a)) and for the "exploitated-state" (Fig. 6(b)). We use the same "exploitation model" as in case "A" of the previous gravity study (Ishido et al., 1995) to forecast SP change due to geothermal operations.

The natural-state SP distribution in and around the Sumikawa field is characterized by a positive anomaly over the central area of the field and a large-amplitude negative anomaly at Mt. Yake to the south (Ishido et al., 1987). After several trial-and-error parameter adjustment calculations, we obtained a result which reproduces these features of the natural-state SP distribution reasonably well (see Fig 6(a)).

The minimum permeabilities (kmin) for the various rock formations used in Eq. 5 and the Rev function (Eq.6) were the important free parameters adjusted during the trial-and-error process. Large discontinuities in permeability will cause large values of the computed Idrag (Eq. 5) in the presence of pressure gradients

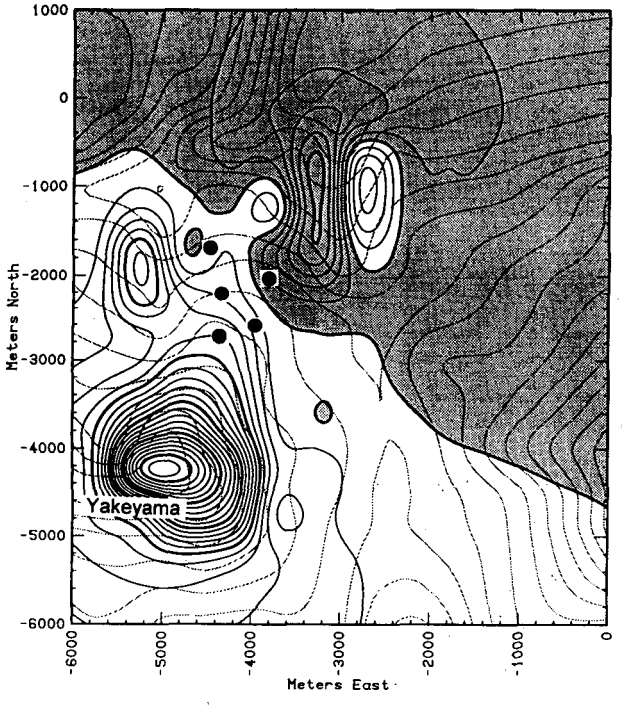


Fig. 6 (a). Calculated self-potential distribution for the natural-state model of the Sumikawa field. Contour interval is 5 mV (SP is positive in shaded area).

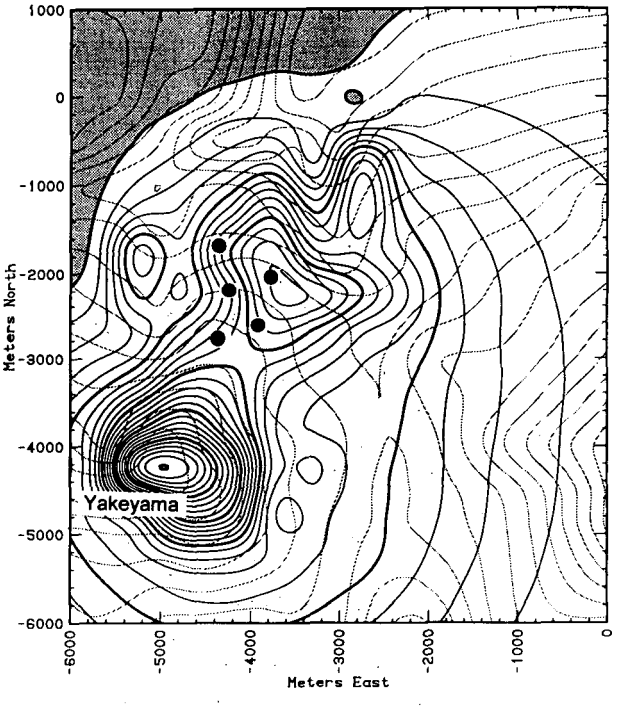


Fig. 6 (b). Prediction of SP distribution after 5 years of 50 MWe production. Drilling pads are shown by solid circles.

(such as the interface between the reservoir and the caprock); in reality, local heterogeneities appear to homogenize this effect. For such regions, we therefore set kmin comparable to the reservoir permeability for the caprock blocks, which seems to remove these synthetic current sources. We set Rev equal to 1 for all liquid saturations larger than the residual saturation; this means Idrag is not reduced for two-phase flow (containing vapor phase which cannot move charge) so long as the liquid phase flows. If we assume Rev = RL (relative permeability of liquid phase), the positive anomaly over the Sumikawa field becomes much smaller both in magnitude and in spatial extent. Other important adjustments were made regarding the selection of the proper mixing law for pore-fluid conductivity and Lee estimation to reproduce the observed conductivity distribution in the field.

The SP distribution during exploitation was then calculated using the same parameter set as that obtained during the natural-state modeling. As shown in Fig. 6(b), a negative anomaly appears over the central area, replacing the positive anomaly of the natural state. This prediction is partly confirmed by the measurements (Matsushima et al., 1995) carried out in 1993, while a long-term field-wide discharge test was going on as a preparatory operation to the start-up of the Sumikawa geothermal power station (50 MWe) in March 1995. The negative anomaly is thought to be caused by pressure drawdown taking place near the bottom of the two-phase zone, where the streaming potential coefficient (C=-Lev/Lee) changes steeply. This mechanism can also be interpreted based upon the total potential approach.

## CONCLUDING REMARKS

In addition to electrokinetic (EK) coupling, several effects such as thermoelectric coupling and chemical diffusion potential are possible causes of self-potential anomalies in geothermal fields. The results of the present simulations, however, indicate that EK effects are the main cause of natural-state SP anomalies associated with vigorous hydrothermal convection.

As the development of a field takes place, the natural flow pattern is likely to be overwhelmed by perturbations caused by the production and injection wells. This will bring about changes in the self-potential distribution through EK coupling. No other effects will play significant roles, since production-induced changes in the distributions of temperature and fluid chemistry will be minor compared to flow pattern changes, especially in the early stages of exploitation. The present results support this observation. Repetitive self-potential surveying of geothermal fields during exploitation would appear to be another promising tool for field monitoring (along with other types of monitoring such as downhole pressure and temperature measurements and surface microgravity surveys), to provide better reservoir models and more effective field management.

## REFERENCES


Anderson, L.A. and Johnson, G.R. (1976), " Application of the Self-potential Method to Geothermal Exploration in Long Valley, California," J. Geophys. Res., **81**, 1527-1532.

Combs , J. and Wilt, M.J. (1976), "Telluric Mapping, Telluric Profiling, and Self-potential Surveys of the Dunes Geothermal Anomaly, Imperial Valley, California, " in Proc. 2nd U.N. Symposium on the Development and Use of Geothermal Resources, vol.2, 937-945.

Corwin, R.F. and Hoover, D.B. (1979), " The Self-potential Method in Geothermal Exploration," Geophysics, **44**, 226-245.

de Groot, S.R. and Mazur P. (1962), "Non-equilibrium Thermodynamics," North-Holland, Amsterdam, pp 405-452.

Fitterman, D.V. (1978), " Electrokinetic and Magnetic Anomalies Associated with Dilatant Regions in a Layered Earth," J. Geophys. Res., **83**, 5923-5928.

Ishido, T. (1981), " Streaming Potential Associated with Hydrothermal Convection in the Crust: a Possible Mechanism of Self-potential Anomalies in Geothermal Areas," Journal of Geothermal Research Society of Japan, **3**, 87-100 (in Japanese with English abstr.).

Ishido, T. (1989), "Self-potential Generation by Subsurface Water Flow Through Electrokinetic Coupling," in Detection of Subsurface Flow Phenomena, Lecture Notes in Earth Sciences, v. 27, G.-P. Merkler et al. (Eds.), Springer-Verlag , pp 121-131..

Ishido, T., Kikuchi, T. and Sugihara, M. (1987), "The Electrokinetic Mechanism of Hydrothermal-circulation-related and Production-induced Self-potentials," in Proc. 12th Workshop on Geothermal Reservoir Engineering, Stanford University, 285-290.

Ishido, T., Kikuchi, T., Yano, Y., Sugihara, M. and Nakao, S. (1990), "Hydrogeology Inferred from the

Self-potential Distribution, Kirishima Geothermal Field, Japan," GRC Transactions, vol.14-part II, 916-926.

Ishido, T. and Mizutani, H. (1981), " Experimental and Theoretical Basis of Electrokinetic Phenomena in Rock-water Systems and its Applications to Geophysics," J. Geophys. Res., **86**, 1763-1775.

Ishido, T., Mizutani, H., and Baba, K.(1983), " Streaming Potential Observations, Using Geothermal Wells and in situ Electrokinetic Coupling Coefficients Under High Temperature," Tectonophysics, **91**, 89-104.

Ishido, T., Sugihara, M., Pritchett, J.W. and Ariki, K. (1995), "Feasibility Study of Reservoir Monitoring Using Repeat Precision Gravity Measurements at the Sumikawa Geothermal Field," in Proc. World Geothermal Congress, Florence, 853-859.

Matsushima, N., Yano, Y., Kikuchi, T. and Ishido, T. (1995), "Self-potential Measurements at the Sumikawa Geothermal Field," in Interim Report of New Sunshine Project: Research on Exploration Technology of Deep Geothermal Resources, Geological Survey of Japan, 81-105.

Mizutani, H., Ishido, T., Yokokura, T., and Ohnishi, S. (1976), "Electrokinetic Phenomena Associated with Earthquakes," Geophys. Res. Lett., **3**, 365-368.

Morgan, F.D., Williams, E.R. and Madden, T.R. (1989), "Streaming Potential Properties of Westerly Granite with Applications," J. Geophys. Res., **94**, 12449-12461.

Nourbehecht, B. (1963), "Irreversible Thermodynamic Effects in Inhomogeneous Media and their Applications in Certain Geoelectric Problems," Ph.D. thesis, M.I.T.

Ogilvy, A.A., Ayed, M.A. and Bogoslovsky, V.A. (1969), "Geophysical Studies of Water Leakages from Reservoirs," Geophysical Prospecting, **17**, 36-62.

Olhoeft, G.R. (1981), "Electrical Properties of Rocks," in Physical Properties of Rocks and Minerals, Touloukian, Y.S., W.R.Judd and R.F.Roy (Eds.), McGraw-Hill, New York, pp 257-329.

Pritchett, J.W. (1989), "STAR Users Manual," S-Cubed Report SSS-TR-89-10242.

Pritchett, J.W. (1995), "STAR: a Geothermal Reservoir Simulation System," in Proc. World Geothermal Congress, Florence, 2959-2963.

Pritchett, J.W., Garg, S.K., Ariki, K. and Kawano, Y. (1991), "Numerical Simulation of the Sumikawa Geothermal Field in the Natural State," in Proc. 16th Workshop on Geothermal Reservoir Engineering, Stanford University, 151-158.

Quist, A.S. and Marshall, W.L. (1968), "Electrical Conductances of Aqueous Sodium Chloride Solutions from 0 to 800 Degrees and at Pressures to 4000 bars," J.Phys.Chem., **72**, 684-703.

Sill, W.R. (1983), "Self-potential Modeling from Primary Flows," Geophysics, **48**, 76-86.

Wurmstich, B. and Morgan, F.D. (1994), "Modeling of Streaming Potential Responses Caused by Oil Well Pumping," Geophysics, **59**, 46-56.

Yasukawa, K., Bodvarsson, G.S. and Wilt, M.J. (1993), "A Coupled Self-potential and Mass-Heat Flow Code for Geothermal Applications," in GRC Transactions, vol.17, 203-207.

Zablocki, C.J. (1976), "Mapping Thermal Anomalies on an Active Volcano by the Self-potential Method, Kilauea, Hawaii," in Proc. 2nd U.N. Symposium on the Development and Use of Geothermal Resources, vol. 2, 1299-1309.

Zohdy, A.A.R., Anderson, L.A. and Muffler, L.J.P. (1973), " Resistivity, Self-potential, and Induced-polarization Surveys of a Vapor-dominated Geothermal System," Geophysics, **38**, 1130-1144.